Cancer Letters 639 (2026) 218235

Contents lists available at ScienceDirect

Cancer Letters

journal homepage: www.elsevier.com/locate/canlet

Original Articles

Anti-BCMA-CAR-IL15 natural killer cells prevent multiple myeloma growth in the bone marrow but allow subsequent emergence of extramedullary disease

Shelby Kaczmarek [a,b], Donghyeon Jo [a,b], Safa Ghaziasgar [a,b], Bryan Marr [a,b], Stefania Berton [a,b], Lisheng Wang [a,b,c], Mehdi Arbabi Ghahroudi [a,d], Mihue Jang [e,f], Alissa Visram [g], Scott McComb [a,b,c,d], Seung-Hwan Lee [a,b,c,*]

[a] Department of Biochemistry, Microbiology, and Immunology (BMI), Faculty of Medicine, University of Ottawa, Ottawa, ON, Canada
[b] Centre for Infection, Immunity, and Inflammation (CI3), Faculty of Medicine, University of Ottawa, Ottawa, ON, Canada
[c] The Ottawa Institute of Systems Biology (OISB), Faculty of Medicine, University of Ottawa, Ottawa, ON, Canada
[d] Human Health Therapeutics Research Centre (HHT), National Research Council of Canada, Ottawa, ON, Canada
[e] Medicinal Materials Research Center, Biomedical Research Division, Korea Institute of Science and Technology, Seoul, South Korea
[f] KHU-KIST Department of Converging Science and Technology, Kyung Hee University, Seoul, South Korea
[g] Department of Oncology, Juravinski Cancer Center, McMaster University, Hamilton, ON, Canada

ARTICLE INFO

Keywords:
Multiple myeloma
Chimeric antigen receptor
Natural killer cells
BCMA-CAR
Extramedullary disease
Plasmacytomas

ABSTRACT

Multiple myeloma (MM) is an aggressive blood cancer arising from plasma cells. B cell maturation antigen (BCMA)-directed chimeric antigen receptor T cell (α-BCMA-CAR-T) immunotherapies currently provide life-saving treatment for MM patients. Unfortunately, the high cost and manufacturing complexity of autologous CAR-T therapy remain important limitations. Novel research is underway to use CAR-expressing natural killer (NK) cells as an allogeneic CAR-T alternative, but studies have yet to evaluate long-term CAR-NK efficacy against MM. In this study, NK cells were isolated, expanded via feeder-cell stimulation, and engineered to express α-BCMA-CAR with or without human IL-15 co-expression using lentiviral vectors. In a xenograft model, both α-BCMA-CAR and IL-15 expression were required for persistent restriction of MM growth in the blood and bone marrow. Despite near complete and sustained elimination of MM in the bone marrow, long-term assessment of mice treated with α-BCMA-CAR-IL15 NK cells revealed the emergence of extramedullary disease (EMD) in the form of BCMA-positive MM plasmacytomas. This study showcases α-BCMA-CAR-IL15 NK cell therapy as a potent anti-MM therapeutic, achieving sustained MM elimination from the bone marrow and greatly extending survival. However, α-BCMA-CAR-IL15 NK cells appeared ineffective at eliminating extramedullary disease. By demonstrating the strengths and weaknesses of α-BCMA-CAR-IL15 cells, we hope this study could help direct the use of such therapies in clinical trials and provide a valuable pre-clinical MM model for studying and developing interventions for aggressive MM-EMD.

1. Introduction

Multiple myeloma (MM) is an incurable hematological cancer caused by the malignant transformation of plasma cells, resulting in various clinical presentations attributed to unregulated plasma cell proliferation in the bone marrow and hyper-production of antibodies, including bone destruction, infections, anemia, kidney failure and hypercalcemia. Firstline treatments include combinations of immunomodulatory drugs, proteasome inhibitors, and/or anti-CD38 monoclonal antibodies [1–3]. These regimens have increased patient survival from 4 to 8 years [4]. Despite these advances, patients with disease refractory to the three main drug classes have dismal outcomes, with a median overall survival of approximately 1 year [5], necessitating improved treatment strategies.

The B cell maturation antigen (BCMA) plays a crucial role in B cell differentiation [6]. It is highly expressed on MM compared to healthy

* Corresponding author. Department of Biochemistry, Microbiology & Immunology, Faculty of Medicine, University of Ottawa, Ottawa, Ontario, K1H 8M5, Canada.
E-mail address: seunglee@uottawa.ca (S.-H. Lee).

https://doi.org/10.1016/j.canlet.2025.218235
Received 30 July 2025; Received in revised form 14 December 2025; Accepted 23 December 2025
Available online 24 December 2025

plasma cells, making BCMA an optimal immunotherapeutic target [7]. T cells expressing anti-BCMA chimeric antigen receptors (α-BCMA-CAR-T) have been FDA-approved since 2021 for the treatment of MM with an overall response rate of 73–98 % [8,9]. However, CAR-T therapy continues to pose financial, social and logistical barriers that limit universal patient access [10,11]. In addition, the high cost and lengthy manufacturing time for available autologous α-BCMA-CAR-T therapies ide-cel (median 47 days, range 34–91) and cilta-cel (median 70 days, range 36–275) [12,13] severely restricts access for patients with aggressive disease who do not have adequate bridging therapies.

Natural killer (NK) cells may be an attractive CAR-T alternative due to their established safety in allogeneic clinical trials [14] with the potential to generate universal, cost-effective "off-the-shelf" immunotherapies from healthy donors [15]. NK cells have diverse receptors which can recognize tumour cells that downmodulate human leukocyte antigens (HLA) ligands for immune escape [15]. Recent studies have shown that MM can suppress NK cell-mediated anti-myeloma activity by upregulating HLA-C and HLA-E expression [16–18]. Furthermore, NK cells require IL-2 and/or IL-15 cytokine stimulation to support their *in vivo* persistence [19]. Cytokine and CAR encoding sequences can be incorporated together in multi-expression constructs to enhance the persistence or function of CAR-expressing cells without exogenous administration of cytokines [20,21], as was done for an α-CD19-CAR-IL15 clinical trial [22]. In this study, we perform long-term *in vivo* assessment of α-BCMA-CAR NK cells with or without IL-15 expression, demonstrating that both CAR and IL-15 are required for NK persistence and the effective inhibition of MM growth in the blood and bone marrow. Notably, despite effective restriction in the bone marrow, we observe a late onset of BCMA-positive tumour masses, consistent with extramedullary disease (EMD), which is predominantly observed in relapsed MM patients [23]. This report highlights both the strengths and weaknesses of α-BCMA-CAR-IL15 NK cell therapy, providing critical insights for CAR-NK clinical development and a research platform to explore next-generation or combinatorial therapies to target MM-EMD.

2. Methods

2.1. Culture of human cell lines

NALM6 (ATCC) and MM.1S (ATCC, gifted by Dr. Michele Ardolino) cell lines were cultured in RPMI-1640 media (350-000-CL; Wisent) containing 10 % HI-FBS (12484028; Gibco), 100 μg/mL Pen/Strep (SV30010; Hyclone), 55 μM β-Mercaptoethanol (21985023; Gibco), and 20 mM HEPES (CA12001-708; VWR) (hereafter called RP10 media). Lenti-X 293T cells (632180; Takara) were cultured with 10 % HI-FBS and 100 μg/mL Pen/Strep supplemented High-Glucose DMEM media (319-005-CL; Wisent). NK92 cells were cultured in RP10 supplemented with 200 U/mL human recombinant IL-2 (NCI Preclinical Repository, USA).

2.2. Isolation and production of a human primary NK (pNK) cell master stock

Healthy adult blood collection was approved by the Ottawa HSNR Ethics Board (#20200527-01H) and the University of Ottawa (#H-01-21-6568). Peripheral blood mononuclear cells (PBMC) were isolated by Ficoll gradient centrifugation as previously described [24]. Primary NK cells were isolated by negative magnetic selection using the MojoSort human NK cell isolation kit (480054; Biolegend) and plated in RP10 supplemented with 100 U/mL IL-2. pNKs were immediately stimulated 1:2 with irradiated membrane-bound IL-21 and 4-1BBL-expressing K562 feeder cells [25] (gifted from CYTOSEN) and expanded for 7 days based on a previously reported protocol [26]. The partially expanded pNK cells (hereafter called master stock) were frozen at −80 °C with freezing media containing 90 % HI-FBS and 10 % DMSO (BP231-100; FisherBioReagents).

2.3. Plasmid construction

CAR constructs incorporated a BCMA-specific camelid nanobody (VHH) binding element generated via immunization of an adult *llama glama* and phage panning against human BCMA extracellular domain fused to a VHH carrier, similarly to previously reported [27,28]. The α-BCMA-VHH (clone A6) was then integrated into a lentiviral plasmid along with a human CD8-hinge domain, CD28-transmembrane domain, and both 4-1BB and CD3ζ signaling domains to make the CAR sequence. In addition, either a NeonGreen fluorescent tag or human IL-15 cytokine was linked to the CAR via a P2A sequence. The amino acid sequences for α-BCMA-CAR with or without IL-15 can be found in Supplementary Table S1. A control GFP-IL15 lentiviral plasmid was also generated. The baboon envelope retroviral glycoprotein (BaEV-TR) was chosen to efficiently transduce NK92 and primary NK cells [29,30], and was cloned as previously described [24].

2.4. Lentivirus production

Lentivirus was produced as previously described [24]. Briefly, Lenti-X 293T cells were transfected using Lipofectamine 3000 (L3000015; Invitrogen) with 1,200 ng of transfer plasmids, 1,200 ng of psPAX2 (gifted from Didier Trono; 12260; Addgene), and 160–200 ng of BaEV-TR. 48- and 96-h viral supernatant was collected, filtered and frozen at −80 °C.

2.5. NK92 cell transduction

Functional lentivirus titer was estimated by transducing NK92 cells with serial dilutions of virus as previously described [24]. NK92 cells were transduced using a virus MOI of 1–2 as previously described [24]. α-BCMA-CAR NK92 cells were sorted based on CAR^+ $EGFP^+$ expression using the SH800 (Sony) at the University of Ottawa (uOttawa) flow core. GFP-IL15 and α-BCMA-CAR-IL15 NK92 cells were selected for transduced populations by culturing the cells without IL-2.

2.6. pNK cell transduction and expansion

Master stock pNK cells were thawed and rested overnight in RP10 media containing 100 U/mL IL-2. The next day, pNKs were transduced with virus (MOI 2–5) in a Retronectin-coated 48-well flat-bottom plate with Opti-MEM media supplemented with 5 % HI-FBS and 200 U/mL IL-2. The cells were spun down at 1200×*g* for 30 min at 32 °C and cultured overnight at 37 °C and 5 % CO_2. The next day, cells were resuspended in NKMACS (130-114-429; Miltenyi Biotec) supplemented with 10 % HI-FBS, 100 μg/mL Pen/Strep and 100 U/mL IL-2 and were stimulated with 5x more irradiated feeder cells. Throughout expansion, NKMACS media was replaced every 2–3 days. pNKs were stimulated 1:2 with feeder cells after 7 days, followed by expansion for another 5 days. Fully expanded NK cells (21 days from PBMC isolation, 13 days after transduction) were used for *in vitro* assays and *in vivo* studies (Supplementary Fig. S1).

2.7. Immunostaining

Refer to supplemental methods for a list of antibodies and viability dyes used, as well as surface and intracellular immunostaining protocols. Anti-VHH (Alexa-Fluor647-CAR) antibody was generated at the NRC [31].

2.8. NK cell functional assays

5×10^4 NK cells were incubated with NALM6 or MM.1S target cells at an E:T ratio of 1:3 in a 96-well U-bottom plate. GolgiPlug (555028;

BD) or anti-CD107a antibody was added immediately during plating for IFNγ or CD107a measurement, respectively. After 4 h of co-incubation, cells were stained with anti-CD56, anti-CAR, live/dead fixable dye for NK92 cells and anti-CD56, live/dead fixable dye for pNK cells. Intracellular IFNγ proteins were fixed and stained with an anti-IFNγ antibody according to the manufacturer's protocol (555028, BD).

2.9. IncuCyte cytotoxicity assays

1×10^5 NuclightRED MM.1S cells were incubated with E:T ratios of 0.3:1 for NK92 and 0.5:1 for pNK cells in a 96-well flat-bottom plate. The cells were imaged using phase, green and red channels every 2 h at 10× magnification using IncuCyte S3 (Satorius). The red fold change was calculated using the equation below. (Fluor: Fluorescence, t: time)

$$\frac{Fluor_{t=x}}{Fluor_{t=0}}$$

2.10. Cytokine depletion viability assays

2.5×10^4 NK92 or primary NK cells were seeded in a 24-well plate with RP10 or NKMACS, respectively. After 3 and 5 days, an aliquot was taken for immunostaining with anti-CD56, anti-CAR, and live/dead fixable dye. Viability was gated on $EGFP^+$ or CAR^+ cells when transduced.

2.11. In vivo multiple myeloma models

NOD.Cg-Prkdc^{scid} Il2rg^{tm1Wjl}/SzJ (NSG) mice (Jackson Laboratories) were maintained in a pathogen-free animal facility at uOttawa following Canadian Council on Animal Care regulations. NSG female mice (8–14 weeks old) received 2.5×10^6 firefly luciferase-expressing MM.1S cells intravenously. Mice received either 5×10^6 total pNKs (n = 5), or 3×10^6 to 4.8×10^6 α-BCMA-CAR-IL15-positive pNK cells (n = 5–10) intravenously 2 days post-MM injection. Leftover pNK cells were immediately frozen in liquid nitrogen for consecutive injection on day 25 post-MM (n = 5). Luciferase signal was measured once a week by injecting 150 mg/kg firefly D-luciferin (122799; PerkinElmer) and imaged using IVIS Spectrum (PerkinElmer) or Newton 7.0 FT500 (Vilber) followed by bioluminescent data analysis using Aura 4.08 (Spectral Instruments Imaging) or Kuant (Vilber), respectively. Mouse blood was taken every 1–2 weeks and weight was measured once per week. Mice were sacrificed based on high luciferase signal ($>3 \times 10^9$ photons/s), movement ability (hind limb paralysis), reactivity, and weight loss (>20 %). Refer to supplemental methods for organ harvesting and cell processing procedures. All procedures were approved by and conducted in accordance with uOttawa animal guidelines.

2.12. Statistical analysis and graph generation

Graphs and statistical analysis were generated using GraphPad Prism 5 (Dotmatics). Two-way analysis of variance (ANOVA) followed by a Bonferroni post-hoc test was used to test the means of multiple groups. One-way ANOVA, followed by Tukey post-hoc test, and unpaired two-tailed *t*-test were used to test the means between two or more groups, respectively. Survival curves were compared using the Log-rank (Mantel-Cox) test. Graphs with log(10) y-axis were transformed to log values before analysis. Where indicated, R software (v.4.4) was used to statistically analyze IVIS tumour burden and weight for more than two groups. Using the lme4 package (v1.1-36), log transformed tumour burden and linear weight loss (normalized to baseline) were modeled using a linear mixed effects model with time as a cubic polynomial interacting with treatment and random intercepts and slopes for repeated measures. Comparisons of group means were conducted with the emmeans package (v1.10.7) using the Tukey post-hoc test. Statistical significance for all analyses was defined as $p < 0.05$.

3. Results

3.1. Anti-BCMA-CAR-IL-15 expression enhances NK92 effector function against myeloma cells

We first generated novel α-BCMA CAR constructs using a modularized CAR plasmid similar to that previously reported [28]. The CAR construct consists of an α-BCMA-VHH [27,28], 4-1BB and CD3ζ signaling domains linked to either a NeonGreen fluorescent tag (α-BCMA-CAR) or the human IL-15 cytokine (α-BCMA-CAR-IL15) via a P2A sequence (Supplementary Table S1). A control GFP-IL15 construct was also generated (**Fig. 1**A). Lentiviral transduction of NK92 cells (Fig. 1B) showed a single population of GFP and CAR with GFP-IL15 and α-BCMA-CAR-IL15 virus, respectively. A double GFP^+/CAR^+ population was observed when transduced with α-BCMA-CAR-GFP, indicating that both CAR and mNeonGreen reporter are well translated under the EFS1α promoter.

We next evaluated the effector function of our engineered NK92 cells against the BCMA-negative leukemia (NALM6) and BCMA-high multiple myeloma (MM.1S) target cell lines (Fig. 1C). IFNγ and CD107a expression of CAR+ NK92 cells was significantly increased compared to CAR- NK92 when co-incubated with the BCMA-high MM.1S cell line (**Fig. 1**D, Supplementary Fig. S2). There was no difference in functional cytokine expression between CAR- and CAR+ NK92 cells when incubated alone or with the BCMA-negative NALM6 control cell line. To assess the cytotoxicity of NK92 cells, we incubated CAR- or CAR+ NK92 cells with BCMA-high MM.1S cells that express NuclightRED and measured the red fluorescence of MM.1S growth over 48 h (Fig. 1E). CAR+ NK92 cells were able to prevent MM.1S growth while there was no significant difference between the growth of MM.1S alone or when incubated with CAR- NK92 cells.

Given the critical role of human IL-15 in NK cell survival and previous clinically successful CAR-NK strategies [22], we investigated whether introducing the human IL-15 gene could maintain NK cell survival *in vitro* without conventional exogenous IL-2 cytokine supplementation. Unmodified (WT) and α-BCMA-CAR NK cells died by D5, whereas GFP-IL15 and α-BCMA-CAR-IL15 NK cells maintained their viability without exogenous cytokine support in the NK92 cell line (Fig. 1F). When IL-15-positive NK92 cells were cultured long-term without IL-2, we saw a preferential selection of transduced NK92 cells (**Supplementary Fig. S3A and B**). Taken together, α-BCMA-CAR-IL-15 expression increases NK92 effector function against multiple myeloma.

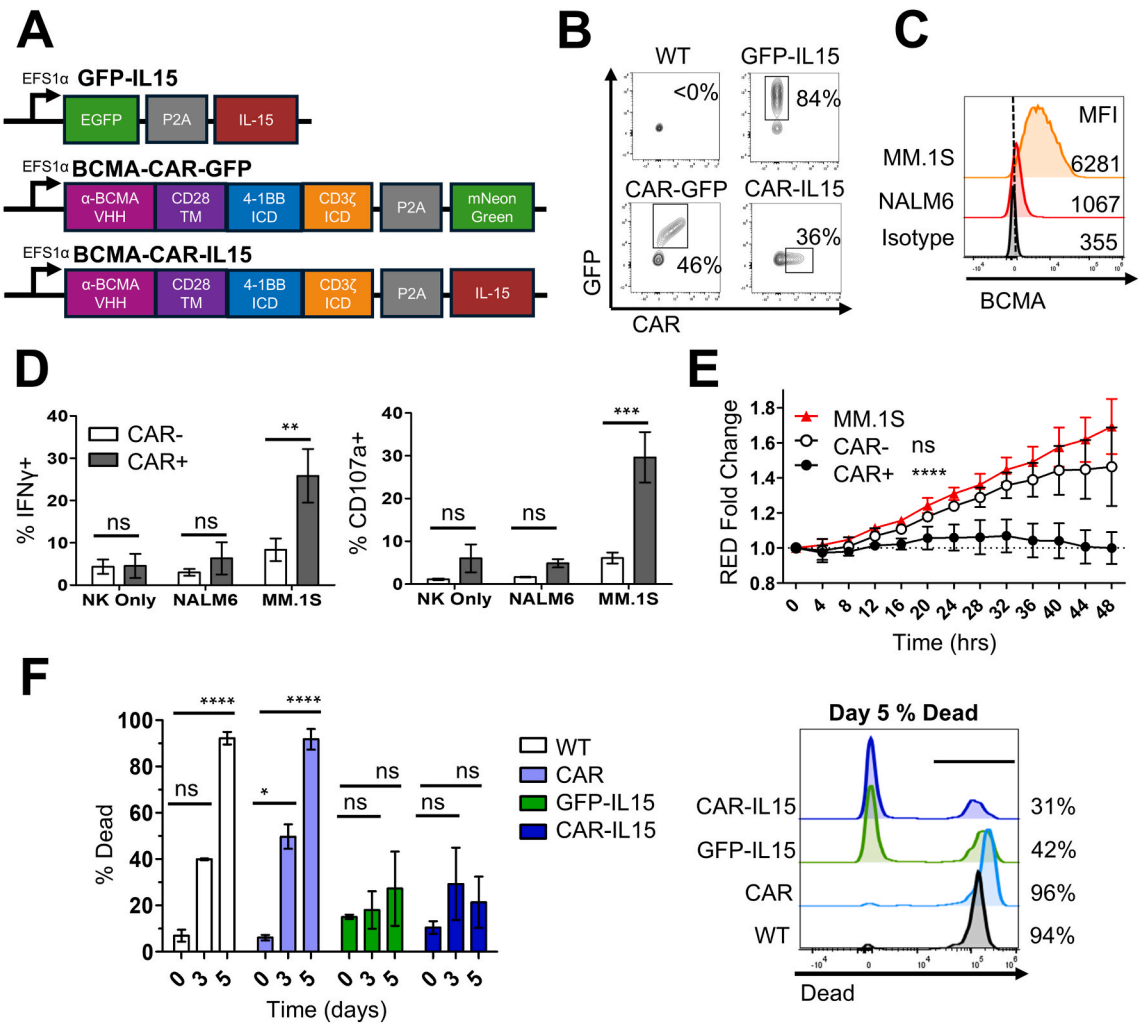

Fig. 1. α-BCMA-CAR-IL15 enhances NK92 effector function and cytotoxicity. (A) The design of GFP-IL15, α-BCMA-CAR and α-BCMA-CAR-IL15 constructs; **(B)** GFP and CAR expression of transduced NK92 cells measured by flow cytometry; **(C)** BCMA expression of target cell lines measured by flow cytometry; **(D)** IFNγ and CD107a functional comparison of α-BCMA-CAR negative (CAR-) or positive (CAR+) NK92 cells against BCMA-neg (NALM6) or BCMA-high (MM.1S) target cells. n = 3 biological replicates; **(E)** The red fluorescent fold change of MM.1S NuclightRED cell growth when incubated with CAR- or CAR+ NK92 cells over 48 h. CAR-/+ groups are compared to the MM.1S target alone. n = 2 biological replicates; **(F)** The viability of NK92 WT or NK92 cells transduced with α-BCMA-CAR, GFP-IL15 or α-BCMA-CAR-IL15 NK92 was assessed over 5 days without exogenous cytokines. n = 2 biological replicates. All data represent mean ± SEM. ns, non-significant; *p < 0.05; **p < 0.01; ***p < 0.001; ****p < 0.0001.

3.2. *Anti-BCMA-CAR-IL-15 expression enhances anti-myeloma activity of primary NK cells*

We next corroborated whether our α-BCMA-CAR construct also augments the effector function of primary NK (pNK) cells against myeloma cells *in vitro*. pNKs were enriched from human PBMCs and expanded for 7 days using irradiated feeder cells and cryopreserved to generate a pNK master stock. Master stock pNKs were thawed, transduced and expanded for an additional 13 days, for a total of 21 days of expansion from PBMC isolation (Supplementary Fig. S1). pNK cells transduced with GFP-IL15 or α-BCMA-CAR-IL15 constructs showed single GFP or CAR populations while α-BCMA-CAR-GFP transduction showed a double GFP^+/CAR^+ population at full expansion (Fig. 2A). Similarly to NK92, CAR+ pNK cells significantly increased IFNγ and CD107a expression compared to untransduced (UT) pNKs when incubated with BCMA-high MM.1S cells, whereas IFNγ and CD107a expression was minimal or non-significant when BCMA-negative NALM6 cells were used (Fig. 2B, Supplementary Fig. S4A). When we assessed primary NK cytotoxicity using the live-cell IncuCyte imager (Fig. 2C, Supplementary Fig. S4B), the growth of MM.1S cells was effectively controlled by CAR+ pNK cells while it remained unaltered when MM cells were incubated alone or with untransduced pNK cells. Interestingly, both UT and CAR+ pNK cells from donor 3 suppressed MM.1S growth, indicating donor-dependent variation in unmodified pNK anti-myeloma cytotoxicity. Consistent with the results observed in NK92 cells, incorporation of the human IL-15 gene protected primary NK cells (from two donors) from cell death *in vitro* without IL-2 (Fig. 2D). Notably, when we compared the anti-myeloma cytotoxicity of primary NKs in the absence of IL-2 over 48 h, only α-BCMA-CAR-IL15 pNK cells effectively controlled MM.1S growth (Supplementary Fig. S5). Overall, these results indicate that α-BCMA-CAR-IL15-expressing NK cells hold strong potential for effective anti-myeloma treatment *in vivo*.

3.3. *α-BCMA-CAR-IL15 pNK cells inhibit myeloma growth while maintaining persistence in vivo*

To evaluate the persistence and anti-myeloma cytotoxicity of α-BCMA-CAR-IL15 pNK cells *in vivo*, we injected 2.5×10^6 MM.1S cells expressing firefly luciferase (MM.1S-FLUC) intravenously (i.v.) into NSG mice. After 2 days post-MM injection, the mice received a single dose of 5×10^6 untransduced (UT), GFP-IL15, α-BCMA-CAR or α-BCMA-CAR-IL15 primary NK cells intravenously (Fig. 3A). GFP and CAR expression

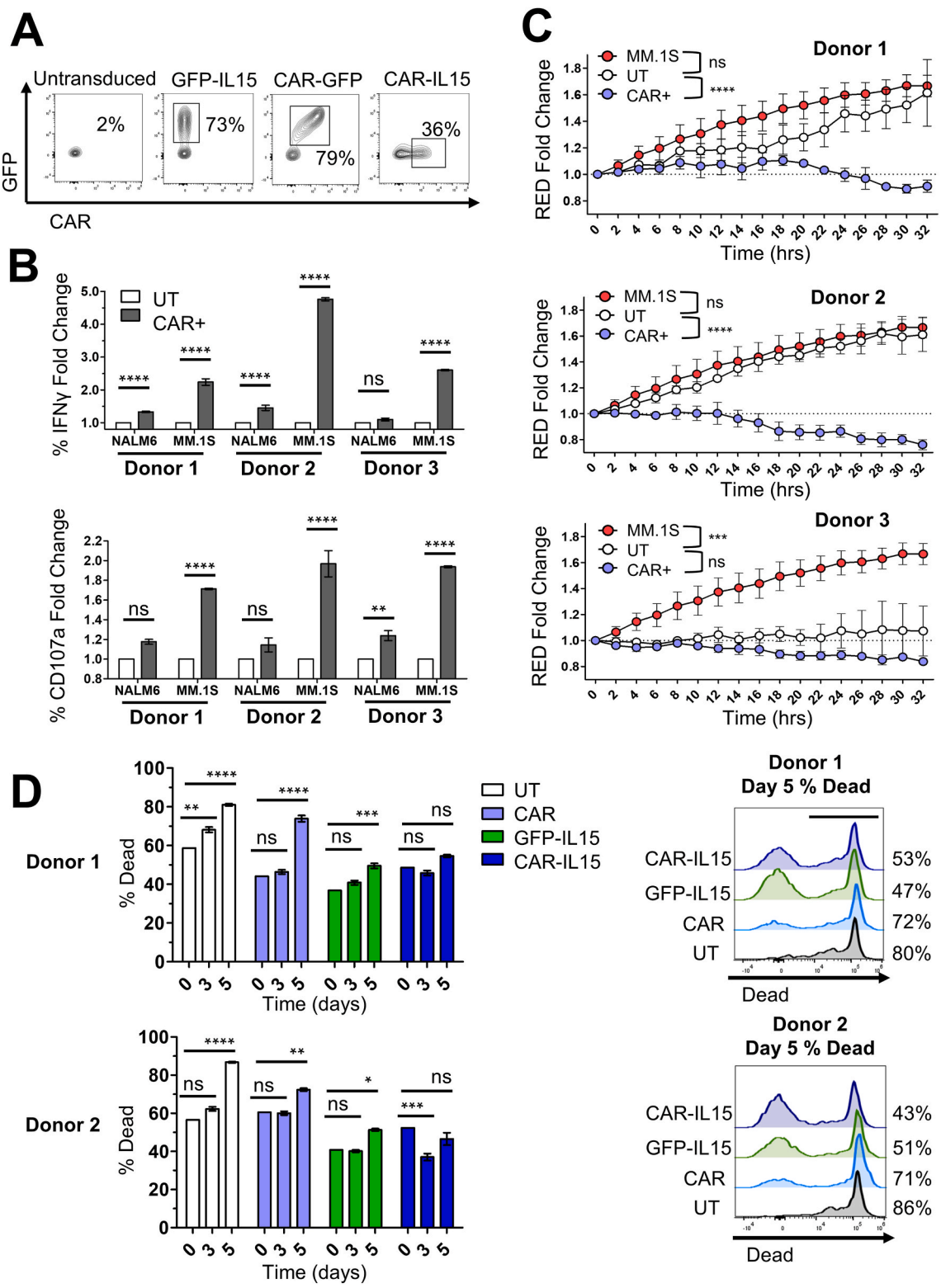

Fig. 2. α-BCMA-CAR-IL15 augments primary NK cell effector function and cytotoxicity *in vitro*. **(A)** GFP and CAR expression of untransduced or transduced primary NK (pNK) cells measured by flow cytometry represented by one donor; **(B)** IFNγ and CD107a functional comparison of untransduced (UT) or α-BCMA-CAR-positive (CAR+) pNKs against BCMA-neg (NALM6) or BCMA-high (MM.1S) target cells. n = 3 donors; **(C)** The red fluorescent fold change of MM.1S NuclightRED cell growth when incubated with UT or CAR+ pNK cells over 32 h. n = 2 donors; **(D)** The viability of untransduced, α-BCMA-CAR, GFP-IL15 and α-BCMA-CAR-IL15 primary NK cells was assessed over 5 days without exogenous cytokines. n = 2 donors. All data represent mean ± SEM. ns, non-significant; *p < 0.05; **p < 0.01; ***p < 0.001; ****p < 0.0001. UT: untransduced.

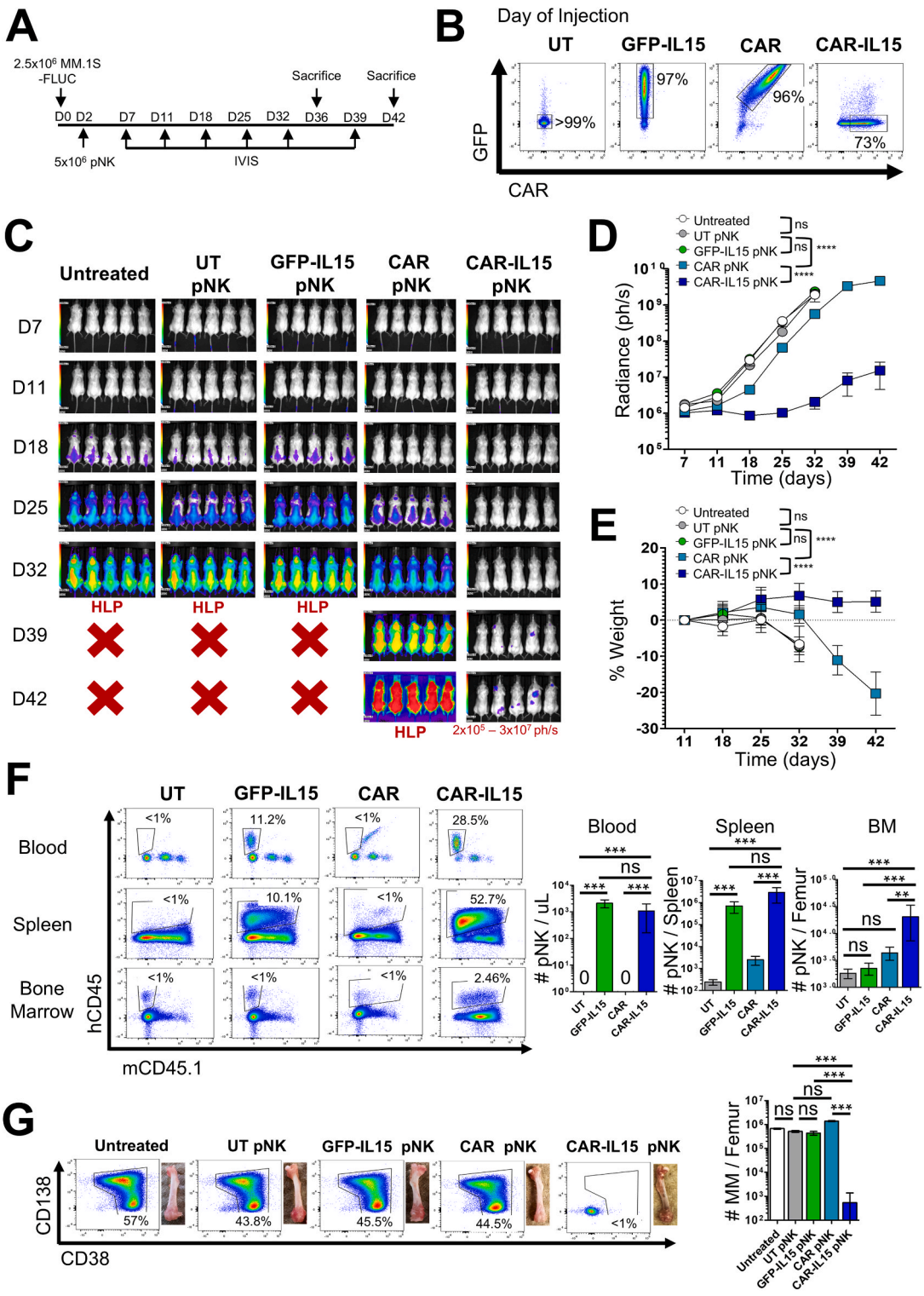

Fig. 3. The anti-myeloma comparison of untransduced, GFP-IL15, α-BCMA-CAR and α-BCMA-CAR-IL15 primary NK cells. (A) Schematic experimental timeline in which 2.5×10^6 luciferase-expressing MM.1S multiple myeloma cells were injected (i.v.) into NSG mice, followed by a single injection (i.v.) of 5×10^6 total untransduced, GFP-IL15, α-BCMA-CAR or α-BCMA-CAR-IL15 primary NK cells 2 days later (n = 5); **(B)** CAR and GFP expression of primary NK cells on the day of injection; **(C–D)** The tumour burden of each group was measured on days 7, 11, 18, 25, 32, 39 and 42 using IVIS and the total bioluminescent signal was quantified. Statistical analysis was performed using R software as described in the methods; **(E)** The percent weight change of mice was monitored weekly. Statistical analysis was performed using R software as described in the methods; **(F)** The phenotype and number of human $CD45^+$ primary NK cells in the blood, spleen and bone marrow at day 36 or 42 endpoint; **(G)** The phenotype and number of MM cells in the bone marrow at day 36 or 42 endpoint. MM cells were identified as $CD38^+/CD138^{mixed}$ after gating on the human CD45 and mouse CD45.1 negative population ($hCD45^-/mCD45.1^-$). Representative images of the mouse femur depicting the colour of the bone marrow at endpoint. The contrast of all femur images was increased by 20 % in PowerPoint. All 5 mice from each group were sacrificed at day 36 or 42 endpoint and lymphocytes were harvested from the blood, spleen and bone marrow for flow staining. All data represent mean ± SD. ns, non-significant; *p < 0.05; **p < 0.01; ***p < 0.001; ****p < 0.0001. D: days; UT: untransduced; HLP: hind-limb paralysis; BM: bone marrow; MM: multiple myeloma.

were confirmed to be >73 % on the day of injection (Fig. 3B). Bioluminescent luciferase signal was measured to assess MM.1S tumour growth (Fig. 3C and D), while mouse weight (Fig. 3E) and mobility assessment (hind limb paralysis, HLP) was used to determine an ethical endpoint. Based on *in vivo* bioluminescent imaging, we observed comparable MM growth localized to the spine, hips, and head of untreated, UT pNK and GFP-IL15 pNK-treated mice starting at day 18 (Fig. 3C and D), whereas MM growth was delayed by 7 days in mice treated with α-BCMA-CAR pNK cells. Importantly, α-BCMA-CAR-IL15 pNK cell treatment nearly completely suppressed MM growth until day 39. Peripheral blood analysis revealed that the number of IL-15-negative pNK cells (UT and α-BCMA-CAR) was negligible, whereas IL-15-expressing pNK cells (GFP-IL15 and α-BCMA-CAR-IL15) expanded ~3.2-fold by the endpoint (Supplementary Fig. S6A). When assessing pNK cell phenotype *in vivo*, we observed a selection of GFP and a gradual decrease in CAR MFI over time (Supplementary Fig. S6B).

Untreated, UT pNK and GFP-IL15 pNK mice reached humane endpoint on day 36, whereas mice treated with α-BCMA-CAR pNK cells reached humane endpoint on day 42 post-MM injection. Mice treated with α-BCMA-CAR-IL15 pNKs did not reach their humane endpoint but were sacrificed on day 42 for comparative analysis. When quantifying $hCD45^+$ and $mCD45.1^-$ pNK cells in the blood, spleen and bone marrow of treated mice at their endpoints, we found a negligible number of IL-15-negative pNK cells in the blood and less than 1×10^3 pNKs per spleen or femur (Fig. 3F). GFP-IL15 and α-BCMA-CAR-IL15 pNK cells were found in similar amounts in the blood and the spleen. Notably, the quantity of α-BCMA-CAR-IL15 pNK cells in the bone marrow at the endpoint was ~4.7-fold more than IL-15-negative BCMA-CAR pNK and 10-fold more than GFP-IL15 pNK-treated mice (Fig. 3F). We found prominent $CD38^+$ and $CD138^{mixed}$ MM populations in the bone marrow of untreated, UT pNK, GFP-IL15 pNK and α-BCMA-CAR pNK-treated groups (Fig. 3G), which was easily noticed by the unusual white colour of the BM within the femur. Remarkably, α-BCMA-CAR-IL15 pNK cells dramatically reduced MM growth when compared with other pNK treatments, which was corroborated by the preservation of healthy red BM. Taken together, a single dose of α-BCMA-CAR-IL15 pNK cells significantly inhibited MM growth *in vivo* and confirms that the inclusion of both CAR and the IL-15 gene is necessary for therapeutic efficacy and *in vivo* persistence of α-BCMA-CAR-IL15 pNK cells.

3.4. α-BCMA-CAR-IL15 pNK treatment prolongs survival but allows for extramedullary disease

Since α-BCMA-CAR-IL15 pNK treatment did not reach the endpoint on day 42, we next sought to assess the anti-myeloma activity of α-BCMA-CAR-IL15 pNK cells over a longer period of time. Similarly as above, MM.1S-FLUC-bearing mice were treated 2 days later with 3×10^6 α-BCMA-CAR-IL15-positive pNKs in separate experiments using two independent pNK donors (Fig. 4A and B). During the course of these experiments, the IVIS imaging system was upgraded from the IVIS Spectrum to Newton 7.0 FT500. In both experiments, untreated mice exhibited rapid MM progression in osseous regions of the spine, hips and head and reached an ethical endpoint due to HLP between day 36 and 38 (Fig. 4C–E). In contrast, α-BCMA-CAR-IL15 pNK treatment inhibited MM growth until day 40, after which localized tumour growth, mostly outside of osseous regions, was observed. Despite the onset of localized tumours in various anatomical regions, treated mice did not show adverse clinical symptoms such as weight loss or hind-limb paralysis, and were sacrificed between day 58 and 73 due to high bioluminescent signal in localized regions or the presence of palpable tumours. At the endpoint of both experiments (Fig. 4F and G), untreated mice were found to have a mix of mouse lymphocyte and MM cells in the blood with >95 % MM cell engraftment in the bone marrow. Remarkably, α-BCMA-CAR-IL15 pNK-treated mice had <5 % MM in blood and <1 % in the bone marrow. These findings suggest that α-BCMA-CAR-IL15 pNKs effectively kill MM in the bone marrow.

At sacrifice, mice were autopsied and a total of 20 extramedullary tumours were found in 13 mice who received α-BCMA-CAR-IL15 pNK treatment (Fig. 4H). In humans, myeloma extramedullary disease is currently divided into two classifications: (1) paraskeletal plasmacytomas (PPs), which are tumour masses in direct contact with the bone and (2) extramedullary plasmacytomas (EMPs), which are soft-tissue tumour masses that result from hematogenous spread without bone contact [32]. From all mice in both experiments, 2 tumours were PPs while 18 were EMPs. The plasmacytomas weighed 1019 ± 897.1 mg and measured 724.8 ± 634.5 mm^3 (Fig. 4I), not exceeding ethical tumour limits for subcutaneous tumour models, except for one mouse. Phenotyping by flow cytometry revealed that 80 ± 17.6 % of the plasmacytomas were MM cells with tumour-infiltrating $CD45^+$ pNK cells present in all samples, with a mean of 1.8 ± 3.1 % (Fig. 4J). Importantly, BCMA expression levels of MM cells within plasmacytoma solid tumours of CAR-NK-treated mice were comparable to MM cells from the bone marrow of untreated mice (Fig. 4K), suggesting that BCMA down-modulation was not the mechanism of tumour evasion. Taken together, α-BCMA-CAR-IL15 pNK treatment readily eliminates MM in the bone marrow, leading to significantly prolonged survival. However, CAR-NK cell treatment failed to prevent the onset of MM extramedullary disease.

3.5. Consecutive α-BCMA-CAR-IL15 pNK treatment does not prevent extramedullary disease

Since we observed MM extramedullary disease six weeks post-MM injection along with CAR downregulation in mice treated with α-BCMA-CAR-IL15 pNK cells (Supplementary Fig. S6B), we reasoned that CAR downregulation might be the primary cause of extramedullary disease development. Thus, we tested whether consecutive α-BCMA-CAR-IL15 pNK treatments could prevent relapse. 4.8×10^6 α-BCMA-CAR-IL15-positive pNKs were injected 2 days post-MM injection, and leftover pNK cells were immediately frozen for future BCMA-CAR-IL15 treatments (Fig. 5A and B). We verified that frozen α-BCMA-CAR-IL15 pNKs still significantly inhibited MM growth, although their efficacy was slightly reduced compared to fresh α-BCMA-CAR-IL15 pNKs (Supplementary Fig. S7A–C). MM growth was monitored and a second α-BCMA-CAR-IL15 pNK treatment was administered before plasmacytomas were detected on day 25 post-MM injection (2x CAR-IL15 pNK) (Fig. 5C and D). Despite the administration of consecutive α-BCMA-CAR-IL15 pNK treatment (2x), there was no difference in MM growth (Fig. 5C and D) or weight (Fig. 5E) compared to the cohort treated only once (1x). Consistent with previous *in vivo* experiments, there was a drastic reduction in MM cells within the bone marrow of CAR-IL15 pNK-treated mice compared to untreated mice at the endpoint; however, there was no significant difference in bone marrow MM cell engraftment between 1x and 2x CAR-IL15 pNK treatment (Fig. 5F). An equal number of plasmacytomas were found with both single or consecutive α-BCMA-CAR-IL15 treatments, with 1/3 being PPs (1x pNK, mouse 4 and 2x pNK, mouse 1) with the remaining being EMPs (Fig. 5G). There was no difference between single or consecutive CAR-IL15 pNK treatments when assessing plasmacytoma weight, volume, MM percent composition

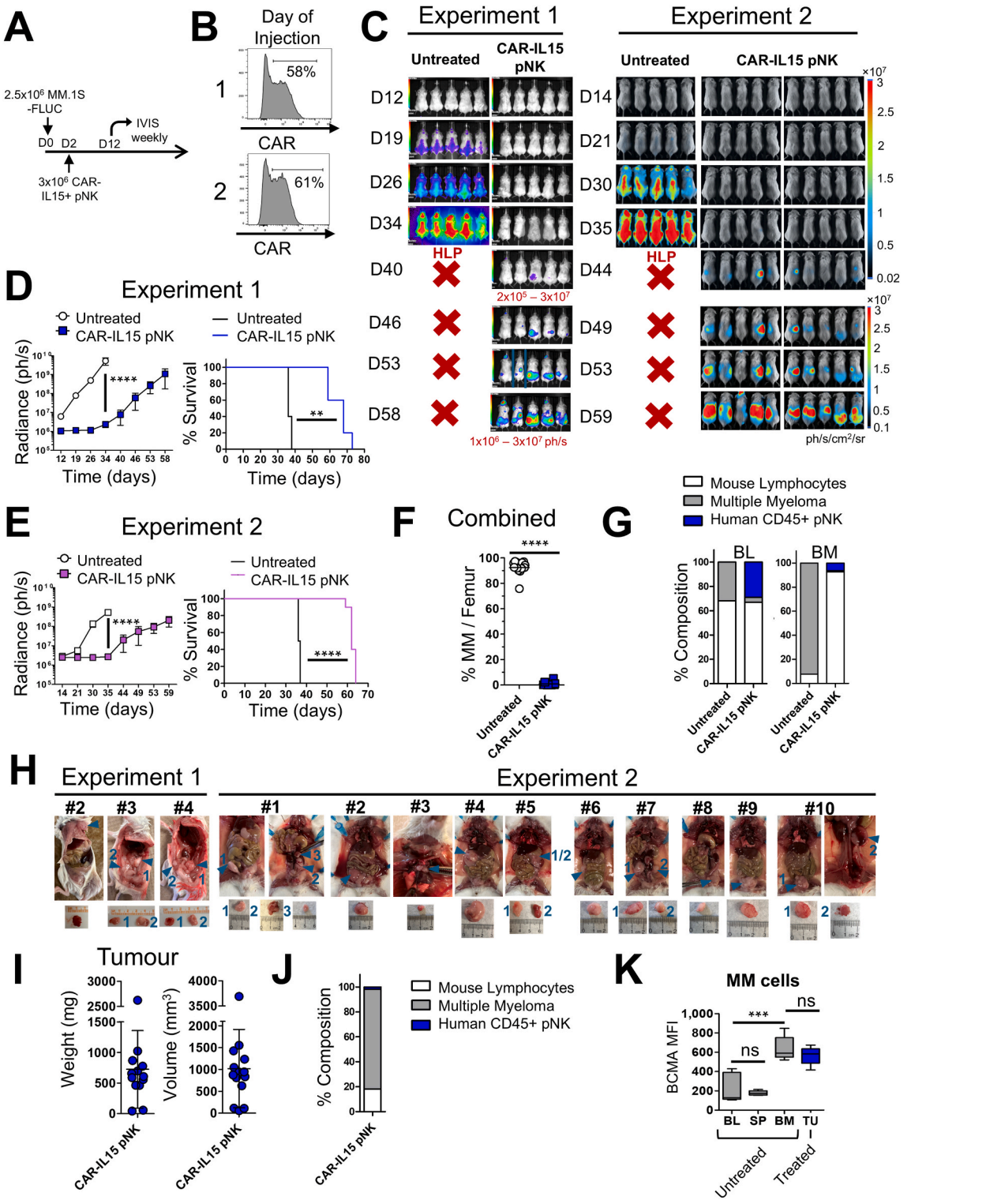

(caption on next page)

Fig. 4. The long-term anti-myeloma cytotoxicity of α-BCMA-CAR-IL15 primary NK cells. (A) Schematic experimental timeline in which 2.5×10^6 luciferase-expressing MM.1S multiple myeloma cells were injected (i.v.) into NSG mice, followed by a single injection (i.v.) of 3×10^6 α-BCMA-A6-CAR-IL15-positive primary NK cells 2 days later; **(B)** CAR expression of primary NK cells from two donors on the day of injection; **(C)** The tumour burden from two separate experiments were measured weekly using IVIS and the total bioluminescent signal was quantified. Mouse 2, experiment 1 on day 53 was not injected with firefly-luciferin properly during initial imaging. It was re-injected and imaged separately on the same day; **(D–E)** The total bioluminescent signal over time and the percent survival of mice from two experiments. Mice were sacrificed between day 58 and 73 (median survival: 68 days in experiment 1, 62 days in experiment 2); **(F)** The percentage of MM cells in the bone marrow at mouse endpoint combined from both untreated and α-BCMA-CAR-IL15 pNK-treated experiments. MM cells were identified as $CD38^+/CD138^{mixed}$ after gating on the human CD45 and mouse CD45.1 negative population ($hCD45^-/mCD45.1^-$); **(G)** Percent composition of mouse lymphocytes ($mCD45.1^+$), multiple myeloma cells ($CD38^+/CD138^{mixed}$), and pNK cells ($hCD45^+$) in the blood and bone marrow at endpoint combined from both experiments. α-BCMA-CAR-IL15 pNK-treated mice had <5 % MM in blood and <1 % in the bone marrow, with a moderate amount of pNK cells remaining in the blood (28.9 ± 39.7 %); **(H)** Images of tumours identified in α-BCMA-CAR-IL15 pNK-treated mice at endpoint. Mouse number refers to the visualized mice in panel C, starting from left to right of the CAR-IL15 pNK-treated groups; **(I)** Total tumour weight and volume measurements for each mouse; **(J)** Percent composition of mouse lymphocytes ($mCD45.1^+$), multiple myeloma cells ($CD38^+/CD138^{mixed}$), and pNK cells ($hCD45^+$) within the tumours; **(K)** BCMA expression of MM cells from blood, spleen and bone marrow from untreated mice and plasmacytoma tumours from α-BCMA-CAR-IL15-treated mice. Mice were sacrificed on different days depending on when they reached a humane endpoint. All mice were autopsied for plasmacytomas, followed by the collection of lymphocytes from the blood, spleen, bone marrow and plasmacytomas for flow staining with the exception of CAR-IL15-treated mouse #5, experiment 1. All data represent mean ± SD. ns, non-significant; *p < 0.05; **p < 0.01; ***p < 0.001; ****p < 0.0001. D: days; HLP: hind-limb paralysis; BL: blood; SP: spleen; BM: bone marrow; TU: tumour; MM: multiple myeloma.

(>83 %) and BCMA expression (Fig. 5H-J). Taken together, consecutive treatment with CAR-IL15 pNKs was unable to prevent the emergence and growth of plasmacytoma tumours.

4. Discussion

Multiple myeloma (MM) is identified by the uncontrolled proliferation of malignant plasma cells [3]. Despite remarkable improvements in the median survival for patients diagnosed with MM over the past two decades, the relapse rate remains high, emphasizing the need for novel therapies. FDA-approved CAR-T immunotherapies targeting BCMA on MM cells are limited by autologous transfusions, high cost and limited patient access [10,11,33]. Allogeneic α-CD19-CAR NK cells have shown potential in leukemia and lymphoma clinical trials, allowing off-the-shelf treatment with minimal side effects [14,34]. While some α-BCMA-CAR-NK phase I/II clinical trials have started recruitment (Clinical trials: NCT05182073, NCT06045091, NCT06242249, NCT06594211), no long-term *in vivo* MM studies have been reported. In our study, we evaluated both the short and long-term effects of α-BCMA-CAR-IL15 primary NK cells in a MM xenograft mouse model to fully understand the strengths and weaknesses of these newly emerging treatment modalities.

In our *in vivo* MM model with NK cell treatment, we present definitive evidence that both IL-15 and α-BCMA-CAR are essential for effective MM disease control. The increased anti-myeloma activity of CAR-IL15 versus CAR NK cells is corroborated by several studies against various cancers [35–39]. The survival of MM-bearing mice after BCMA-CAR-IL15 NK cells (days 58–73) presented in our study aligns with other BCMA-CAR-NK studies, which also had similar endpoints between days 57–70 [38,39]. Notably, our study is the first to monitor bioluminescent MM growth long-term after CAR-NK treatment. Although IL-15 co-expression promotes CAR-NK cell persistence, we did not observe any toxicity related to uncontrolled expansion of IL-15-expressing CAR-NK cells [37,40]. Notably, CAR downmodulation was observed on persisting IL15-expressing CAR-NK cells in the peripheral blood. Since we designed our construct to express CAR and IL-15 simultaneously, pNK persistence suggests that IL-15 was still produced and utilized by NK cells, but α-BCMA-CAR could no longer be expressed on the cell surface. A similar CAR downmodulation in an α-CD19-CAR T cell product was improved by modifying CAR cytoplasmic residues to prevent lysosomal degradation upon CAR internalization, thereby allowing recycling of CARs back to the cell surface [41]. In addition, we recently showed that treating with the histone deacetylase inhibitor, entinostat (ENT), during NK expansion enhanced α-CD138-CAR expression and improved anti-myeloma function *in vitro* and *in vivo* [42].

Given the remarkable MM inhibition achieved with our α-BCMA-CAR-IL15 treatment, we next assessed the long-term anti-myeloma potential of our therapy. Treatment with α-BCMA-CAR-IL15 NK cells improved survival, but we observed the emergence of extramedullary disease (EMD) as evidenced by localized MM growth in the form of MM plasmacytomas. While we did not observe similar MM-EMD in untreated mice, we believe this is likely due to the rapid MM growth in the bone marrow, leading to a swift decline in mouse condition and hind limb paralysis before such EMD can become apparent. Regardless, this study does show that α-BCMA-CAR-IL15-expressing NK cells have a limitation in controlling MM-EMD specifically. Notably, consecutive α-BCMA-CAR-IL15 NK treatments could not prevent the onset of EMD.

The diagnosis of EMD in the clinic is rapidly increasing due to longer patient survival with modern therapies and improved imaging techniques [43–45]. The incidence of EMD with newly diagnosed MM (NDMM) patients ranges from 0.5 to 6 % whereas relapsed/refractory MM (RRMM) patients range from 3.4 to 15 % [23,32,46–48]. In our *in vivo* mouse model of MM treated with α-BCMA-CAR-IL15 NK cells, EMD developed in 76 % of mice. The majority of long-term *in vivo* studies treating MM-bearing NSG mice with cell-based immunotherapies (NK or T cells) do not show bioluminescent MM growth long-term (<50 days) nor indicate the presence or absence of EMD at sacrifice [39,49–52]. To our knowledge, the study of Thangaraj et al. [53] was the only other long-term study that reported MM-EMD emergence in organs and quantified the number of plasmacytomas at endpoint, though without conducting phenotyping.

The use of immunocompromised NSG mice without a full immune system may limit the clinical translation of our model [54,55]. The function and persistence of CAR-NK cells, as well as the incidence of EMD may not be reflected when transitioning this therapy to the clinic with a human immune system. Unfortunately, current humanized mouse models either limit MM engraftment and fail to re-capitulate MM disease progression and pathology [56,57] or are not readily available [58]. While the gold standard for clinical translation would be a fully humanized multiple myeloma (MM) mouse model incorporating human PBMCs together with matched patient-derived MM cells, obtaining paired samples from the same patient for an autologous setting remains ethically challenging. In addition, patient-derived MM cells typically exhibit low and inconsistent engraftment efficiency within murine bone marrow microenvironments. Instead, xenograft models using immunocompromised mice engrafted with human MM cell lines continue to serve as the standard and practical preclinical platform for evaluating CAR-based immunotherapies [39,49–53,59]. There has been some progress with NSG mice expressing human IL-6 to support a primary MM xenograft model [60] but *ex vivo* expansion of patient-derived MM cells remains limited [61,62].

Recent data from BCMA-CAR-T cell treatments strongly corroborate our results. MM studies following BCMA-directed CAR-T cell therapy indicate roughly 50 % of relapses involve EMD throughout the body in tissues such as the lymph nodes, lungs/pleura, muscles, central nervous

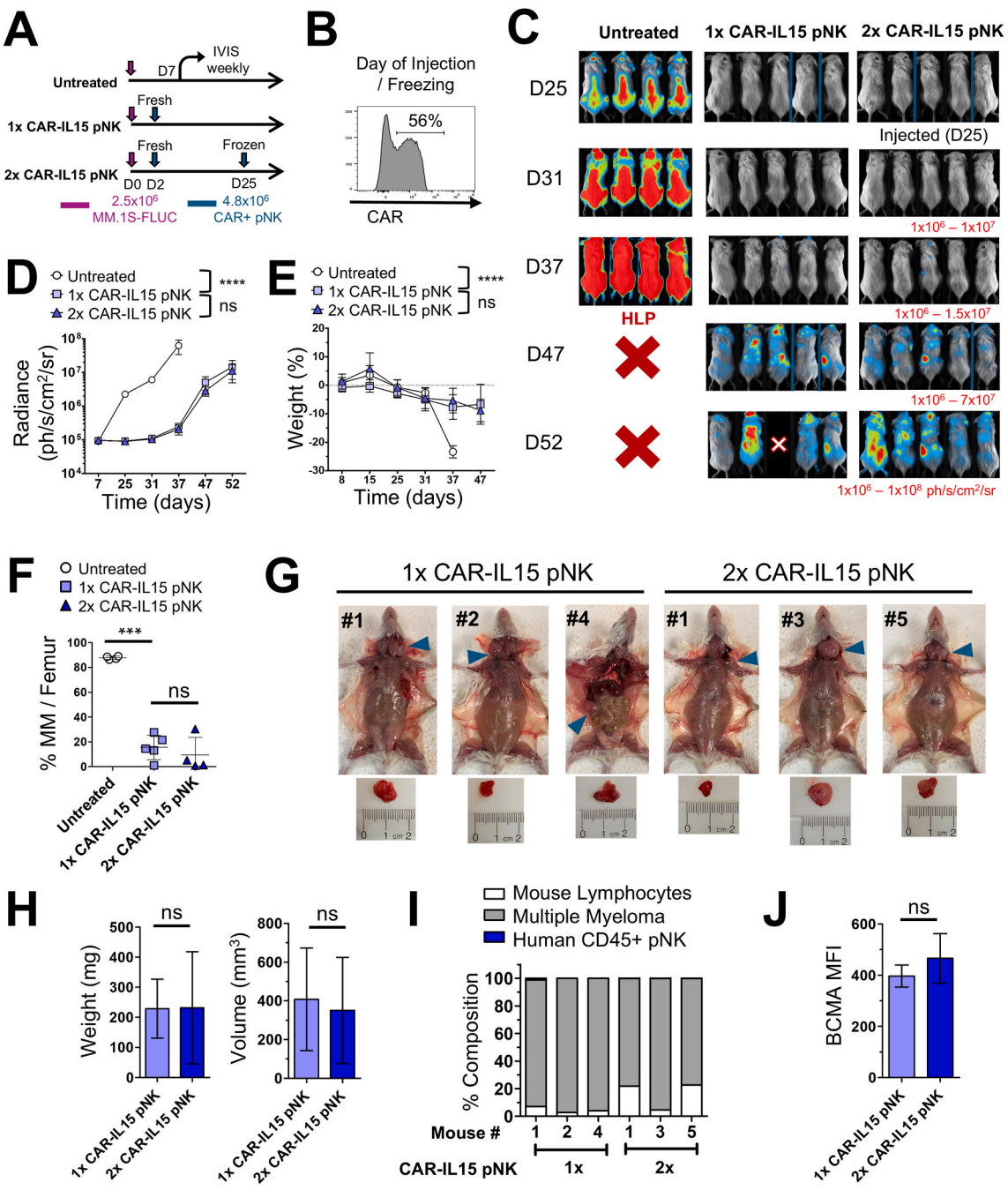

Fig. 5. The anti-EMD comparison of single or consecutive α-BCMA-CAR-IL15 primary NK cell treatment. (A) Schematic experimental timeline in which 2.5 × 10^6 luciferase-expressing MM.1S cells were injected (i.v.) into NSG mice, followed by either a single injection (i.v.) of 4.8 × 10^6 α-BCMA-A6-CAR-IL15-positive primary NK cells 2 days later (1x) or injection (i.v.) of 4.8 × 10^6 α-BCMA-A6-CAR-IL15-positive primary NK cells 2 days and 25 days later (2x) (n = 4 untreated, n = 5 CAR-IL15 pNK); **(B)** CAR expression of primary NK cells on the day of injection; **(C–D)** The tumour burden of each group was measured weekly using IVIS and the mean bioluminescent signal was quantified. α-BCMA-CAR-IL15 pNK-treated mice were imaged on day 25, followed by randomization for the CAR-IL15 NK-treated groups. Bioluminescent images for day 25 are organized into their new groups to follow MM growth progression. **(E)** The percent weight change of mice was monitored weekly; **(F)** The percentage of MM cells in the bone marrow at mouse endpoint. MM cells were identified as $CD38^+/CD138^{mixed}$ after gating on the human CD45 and mouse CD45.1 negative population ($hCD45^-/mCD45.1^-$). **(G)** Images of tumours identified in α-BCMA-CAR-IL15 pNK-treated mice at endpoint. Mouse number refers to the visualized mice in panel C, starting from left to right of the 1x or 2x CAR-IL15 pNK-treated groups; **(H)** Tumour weight and volume measurements for each CAR-IL15 pNK-treated group; **(I)** Percent composition of mouse lymphocytes ($mCD45.1^+$), multiple myeloma cells ($CD38^+/CD138^{mixed}$), and pNK cells ($hCD45^+$) within the tumours. **(J)** BCMA expression of MM cells from tumours of BCMA-CAR-IL15-treated mice. Untreated mice were sacrificed on day 38 and CAR-IL15 pNK-treated mice were sacrificed on day 52–53. 4 untreated, 5 (1x) CAR-IL15 pNK-treated and 4 (2x) CAR-IL15 pNK-treated mice were autopsied for plasmacytomas, followed by the collection of lymphocytes from the bone marrow and plasmacytomas for flow staining. All data represent mean ± SD. ns, non-significant; *p < 0.05; **p < 0.01; ***p < 0.001; ****p < 0.0001. D: days; HLP: hind-limb paralysis; MM: multiple myeloma.

system, ears/nose/throat, gastrointestinal, skin, urinary system and liver [45,63,64]. 43 % of patients with EMD relapse after CAR-T cell therapy remained MM-negative in the bone marrow, showing that bone marrow minimal residual disease (MRD) does not adequately represent overall disease control post-CAR T [64], which is consistent with our results. Moreover, the presence of EMD before CAR-T therapy presents an even greater challenge. Patients with pre-existing EMD have poorer outcomes, including reduced overall response rates, shorter progression-free survival, and lower overall survival [65,66]. EMD is considered an independent adverse prognostic factor which often reflects aggressive disease with high-risk cytogenetics in CAR-T therapy [23,67]. It suggests that extramedullary compartments may serve as an immunosuppressive tumor microenvironment, prohibiting CAR-T cell infiltration, persistence and effector function. Factors such as myeloid-derived suppressor cells, BCMA downregulation, and clonal evolution might contribute to immune escape and resistance [65]. Likewise, in our CAR-NK study, extramedullary tumours showed minimal pNK infiltration (<10 %). Notably, we did not observe BCMA downregulation on EMD-MM cells, indicating that antigen loss is not the primary mechanism driving EMD in our model. Interestingly, a phase 1 trial of bispecific BCMA + GPRC5D CAR-T achieved a 100 % response rate even with all RRMM patients with EMD [68], suggesting that novel strategies such as dual-target CAR constructs might address the challenge of antigen escape in EMD. Moreover, daratumumab (anti-CD38 monoclonal antibodies) [53,69] or bi-specific NK cell engagers (BiKEs) [70,71] could be used in synergistic combination with CAR-NK cells.

In conclusion, α-BCMA-CAR-IL15 primary NK treatment persisted *in vivo* and strongly inhibited MM growth in the bone marrow, with superior efficacy compared to IL15-negative pNKs. Long-term monitoring showed effective restriction of MM growth in the blood and bone marrow with greatly prolonged survival. However, CAR-NK therapy could not limit extramedullary disease relapse. Importantly, this consistent *in vivo* EMD model would offer a valuable opportunity for investigating novel combinational therapies against a highly aggressive form of MM, thereby promoting the development of affordable and accessible immunotherapies for patients.

CRediT authorship contribution statement

Shelby Kaczmarek: Writing – original draft, Visualization, Validation, Methodology, Investigation, Formal analysis, Conceptualization. **Donghyeon Jo:** Resources, Methodology, Investigation. **Safa Ghaziasgar:** Resources, Investigation. **Bryan Marr:** Visualization, Formal analysis. **Stefania Berton:** Writing – review & editing. **Lisheng Wang:** Writing – review & editing. **Mehdi Arbabi Ghahroudi:** Writing – review & editing, Resources. **Mihue Jang:** Writing – review & editing. **Alissa Visram:** Writing – review & editing. **Scott McComb:** Writing – review & editing, Resources, Methodology, Funding acquisition, Conceptualization. **Seung-Hwan Lee:** Writing – original draft, Visualization, Validation, Supervision, Resources, Project administration, Funding acquisition, Formal analysis, Conceptualization.

Ethics approval and consent to participate

Healthy adult blood collection was approved by the Ottawa HSNR Ethics Board (#20200527-01H) and the University of Ottawa (#H-01-21-6568). The mouse colony was housed in the University of Ottawa's specific pathogen-free animal facility, adhering to the Canadian Council on Animal Care guidelines and regulations (BMIb-4430 and BMIe-3392).

Consent for publication

Authors have consent for publication.

Availability of data and material

Data and reagents are available upon reasonable request. All study-related data are either included in the article or provided as online supplementary materials.

Funding

This research was supported by the National Research Council Canada's Disruptive Technology Solutions for Cell and Gene Therapy Challenge Program (CGT-501-2), a Cancer Research Society Grant (#1057810), the National Research Foundation of Korea Grant (#2RS-2024-00509114) and the Canadian Institutes of Health Research (PJT-195765). The International Myeloma Society (IMS) has provided Shelby Kaczmarek with a travel reimbursement to present this data at the 2025 IMS Annual Meeting.

Declaration of competing interest

The authors declare the following financial interests/personal relationships which may be considered as potential competing interests:

Seung-Hwan Lee reports financial support was provided by National Research Council Canada.

Seung-Hwan Lee reports financial support was provided by Cancer Research Society.

Seung-Hwan Lee reports financial support was provided by Canadian Institutes of Health Research.

Seung-Hwan Lee reports financial support was provided by National Research Foundation of Korea.

Seung-Hwan Lee reports equipment, drugs, or supplies was provided by Cytosen Therapeutics.

Seung-Hwan Lee reports equipment, drugs, or supplies was provided by National Cancer Institute Frederick.

Shelby Kaczmarek reports a relationship with International Myeloma Society that includes: travel reimbursement.

Mehdi Arbabi Ghahroudi and Scott McComb has patent #Anti-bcma single domain antibodies and therapeutic constructs; CA3234046A1 pending to National Research Council of Canada.

If there are other authors, they declare that they have no known competing financial interests or personal relationships that could have appeared to influence the work reported in this paper.

Acknowledgements

We thank CYTOSEN for kindly providing the K562 feeder cells expressing 4-1BBL (CD137L) and membrane-bound IL-21 (mbIL-21). The rhIL-2 cytokine was obtained from NCI Preclinical Repository.

Appendix A. Supplementary data

Supplementary data to this article can be found online at https://doi.org/10.1016/j.canlet.2025.218235.

References

[1] S. Kumar, B. Paiva, K.C. Anderson, et al., International Myeloma working group consensus criteria for response and minimal residual disease assessment in multiple myeloma, Lancet Oncol. 17 (2016) e328–e346, https://doi.org/10.1016/S1470-2045(16)30206-6.

[2] S.K. Kumar, V. Rajkumar, R.A. Kyle, et al., Multiple myeloma, Nat. Rev. Dis. Primers 3 (2017) 17046, https://doi.org/10.1038/nrdp.2017.46.

[3] R.A. Kyle, S.V. Rajkumar, Multiple myeloma: ASH 50th anniversary review, Blood 111 (2008) 2962–2972.

[4] S.K. Kumar, S.V. Rajkumar, A. Dispenzieri, et al., Improved survival in multiple myeloma and the impact of novel therapies, Blood 111 (2008) 2516–2520, https://doi.org/10.1182/blood-2007-10-116129.

[5] U.H. Gandhi, R.F. Cornell, A. Lakshman, et al., Outcomes of patients with multiple myeloma refractory to CD38- targeted monoclonal antibody therapy, Leukemia 33 (2019) 2266–2275, https://doi.org/10.1038/s41375-019-0435-7.

[6] B.P. O'Connor, V.S. Raman, L.D. Erickson, et al., BCMA is essential for the survival of long-lived bone marrow plasma cells, J. Exp. Med. 199 (2004) 91–98, https://doi.org/10.1084/jem.20031330.

[7] R.O. Carpenter, M.O. Evbuomwan, S. Pittaluga, et al., B-cell maturation antigen is a promising target for adoptive T-cell therapy of multiple myeloma, Clin. Cancer Res. 19 (2013) 2048–2060, https://doi.org/10.1158/1078-0432.CCR-12-2422.

[8] N.C. Munshi, L.D. Anderson, N. Shah, et al., Idecabtagene vicleucel in relapsed and refractory multiple myeloma, N. Engl. J. Med. 384 (2021) 705–716, https://doi.org/10.1056/nejmoa2024850.

[9] J.G. Berdeja, D. Madduri, S.Z. Usmani, et al., Ciltacabtagene autoleucel, a B-cell maturation antigen-directed chimeric antigen receptor T-cell therapy in patients with relapsed or refractory multiple myeloma (CARTITUDE-1): a phase 1b/2 open-label study, Lancet 398 (2021) 314–324, https://doi.org/10.1016/S0140-6736(21)00933-8.

[10] C. Nze, C.R. Flowers, Barriers to accessing cellular therapy for patients receiving care in community practices, Hematology 2023 (2023) 382–385, https://doi.org/10.1182/HEMATOLOGY.2023000518.

[11] A. Gajra, A. Zalenski, A. Sannareddy, et al., Barriers to chimeric antigen receptor T-Cell (CAR-T) therapies in clinical practice, Pharm. Med. 36 (2022) 163, https://doi.org/10.1007/S40290-022-00428-W.

[12] D.K. Hansen, S. Sidana, L.C. Peres, et al., Idecabtagene vicleucel for relapsed/refractory multiple myeloma: real-world experience from the myeloma CAR T consortium, J. Clin. Oncol. 41 (2023) 2087–2097, https://doi.org/10.1200/JCO.22.01365.

[13] S. Sidana, K.K. Patel, L.C. Peres, et al., Safety and efficacy of standard-of-care ciltacabtagene autoleucel for relapsed/refractory multiple myeloma, Blood 145 (2025) 85–97, https://doi.org/10.1182/BLOOD.2024025945.

[14] D. Marin, Y. Li, R. Basar, et al., Safety, efficacy and determinants of response of allogeneic CD19-specific CAR-NK cells in CD19+ B cell tumors: a phase 1/2 trial, Nat. Med. 30 (2024) 772–784, https://doi.org/10.1038/s41591-023-02785-8.

[15] M.M. Berrien-Elliott, M.T. Jacobs, T.A. Fehniger, Allogeneic natural killer cell therapy, Blood 141 (2023) 856–868, https://doi.org/10.1182/blood.2022016200.

[16] R. Hoteit, A. Bazarbachi, A. Antar, et al., KIR genotype distribution among patients with multiple myeloma: higher prevalence of KIR 2DS4 and KIR 2DS5 genes, Meta Gene. 2 (2014) 730–736, https://doi.org/10.1016/j.mgene.2014.09.008.

[17] D.M. Benson, C.C. Hofmeister, S. Padmanabhan, et al., A phase 1 trial of the anti-KIR antibody IPH2101 in patients with relapsed/refractory multiple myeloma, Blood 120 (2012) 4324–4333, https://doi.org/10.1182/blood-2012-06-438028.

[18] C. Frohn, M. Höppner, P. Schlenke, et al., Anti-myeloma activity of natural killer lymphocytes, Br. J. Haematol. 119 (2002) 660–664, https://doi.org/10.1046/j.1365-2141.2002.03879.x.

[19] B. Becknell, M.A. Caligiuri, Interleukin-2, interleukin-15, and their roles in human natural killer cells, Adv. Immunol. 86 (2005) 209–239, https://doi.org/10.1016/S0065-2776(04)86006-1.

[20] Y. Li, K. Rezvani, H. Rafei, Next-generation chimeric antigen receptors for T- and natural killer-cell therapies against cancer, Immunol. Rev. 320 (2023) 217–235, https://doi.org/10.1111/imr.13255.

[21] M. Chmielewski, H. Abken, TRUCKs: the fourth generation of CARs, Expet Opin. Biol. Ther. 15 (2015) 1145–1154, https://doi.org/10.1517/14712598.2015.1046430.

[22] E. Liu, D. Marin, P. Banerjee, et al., Use of CAR-transduced natural killer cells in CD19-Positive lymphoid tumors, N. Engl. J. Med. 382 (2020) 545–553, https://doi.org/10.1056/nejmoa1910607.

[23] J. Bladé, M. Beksac, J. Caers, et al., Extramedullary disease in multiple myeloma: a systematic literature review, Blood Cancer J. 12 (2022) 1–10, https://doi.org/10.1038/s41408-022-00643-3.

[24] D. Jo, S. Kaczmarek, O. Shin, et al., Simultaneous engineering of natural killer cells for CAR transgenesis and CRISPR-Cas9 knockout using retroviral particles, Mol. Ther., Methods Clin. Dev. 29 (2023) 173–184, https://doi.org/10.1016/j.omtm.2023.03.006.

[25] C.J. Denman, V.V. Senyukov, S.S. Somanchi, et al., Membrane-bound IL-21 promotes sustained Ex vivo proliferation of human natural killer cells, PLoS One 7 (2012), https://doi.org/10.1371/journal.pone.0030264.

[26] S.S. Somanchi, V.V. Senyukov, C.J. Denman, et al., Expansion, purification, and functional assessment of human peripheral blood NK cells, J. Vis. Exp. (2011) 1–5, https://doi.org/10.3791/2540.

[27] M. Arbabi-Ghahroudi, R. Weeratna, S. McComb, et al., Anti-Bcma Single Domain Antibodies and Therapeutic Constructs, 2023. CA3234046A1.

[28] S. McComb, M. Arbabi-Ghahroudi, K.A. Hay, et al., Discovery and preclinical development of a therapeutically active nanobody-based chimeric antigen receptor targeting human CD22, Mol. Ther. Oncol. 32 (2024), https://doi.org/10.1016/J.OMTON.2024.200775.

[29] A.B.L. Colamartino, W. Lemieux, P. Bifsha, et al., Efficient and robust NK-Cell transduction with baboon envelope pseudotyped lentivector, Front. Immunol. 10 (2019), https://doi.org/10.3389/fimmu.2019.02873.

[30] R. Bari, M. Granzin, K.S. Tsang, et al., A distinct subset of highly proliferative and lentiviral vector (LV)-Transducible NK cells define a readily engineered subset for adoptive cellular therapy, Front. Immunol. 10 (2019) 1–12, https://doi.org/10.3389/fimmu.2019.02001.

[31] S. McComb, T. Nguyen, A. Shepherd, et al., Programmable attenuation of antigenic sensitivity for a nanobody-based EGFR chimeric antigen receptor through Hinge domain truncation, Front. Immunol. 13 (2022) 1–16, https://doi.org/10.3389/fimmu.2022.864868.

[32] L. Rosiñol, M. Beksac, E. Zamagni, et al., Expert review on soft-tissue plasmacytomas in multiple myeloma: definition, disease assessment and treatment considerations, Br. J. Haematol. 194 (2021) 496–507, https://doi.org/10.1111/bjh.17338.

[33] W. Qasim, Allogeneic CAR T cell therapies for leukemia, Am. J. Hematol. 94 (2019) S50–S54, https://doi.org/10.1002/ajh.25399.

[34] J.N. Kochenderfer, W.H. Wilson, J.E. Janik, et al., Eradication of B-lineage cells and regression of lymphoma in a patient treated with autologous T cells genetically engineered to recognize CD19, Blood 116 (2010) 4099–4102, https://doi.org/10.1182/blood-2010-04-281931.

[35] E. Liu, Y. Tong, G. Dotti, et al., Cord blood NK cells engineered to express IL-15 and a CD19-targeted CAR show long-term persistence and potent antitumor activity, Leukemia 32 (2018) 520–531, https://doi.org/10.1038/leu.2017.226.

[36] L. Li, V. Mohanty, J. Dou, et al., Loss of metabolic fitness drives tumor resistance after CAR-NK cell therapy and can be overcome by cytokine engineering, Sci. Adv. 9 (2023) 1–15, https://doi.org/10.1126/sciadv.add6997.

[37] I. Christodoulou, W.J. Ho, A. Marple, et al., Engineering CAR-NK cells to secrete IL-15 sustains their anti-AML functionality but is associated with systemic toxicities, J. Immunother. Cancer 9 (2021), https://doi.org/10.1136/jitc-2021-003894.

[38] Q. Ren, Y. Zu, H. Su, et al., Single VHH-Directed BCMA CAR-NK cells for multiple myeloma, Exp. Hematol. Oncol. 12 (2023), https://doi.org/10.1186/S40164-023-00461-8.

[39] Y.Y. Ng, Z. Du, X. Zhang, et al., CXCR4 and anti-BCMA CAR co-modified natural killer cells suppress multiple myeloma progression in a xenograft mouse model, Cancer Gene Ther. 29 (2022) 475–483, https://doi.org/10.1038/s41417-021-00365-x.

[40] G. Tian, A.N. Courtney, H. Yu, et al., Hyperleukocytosis in a neuroblastoma patient after treatment with natural killer T cells expressing a GD2-specific chimeric antigen receptor and IL-15, J. Immunother. Cancer 13 (2025), https://doi.org/10.1136/JITC-2024-010156.

[41] W. Li, S. Qiu, J. Chen, et al., Chimeric antigen receptor designed to prevent ubiquitination and downregulation showed durable Antitumor efficacy, Immunity 53 (2020) 456–470.e6, https://doi.org/10.1016/j.immuni.2020.07.011.

[42] D. Jo, S. Kaczmarek, A. Ul Haq Khan, et al., Entinostat, a histone deacetylase inhibitor, enhances CAR-NK cell anti-tumor activity by sustaining CAR expression, Front. Immunol. 16 (2025), https://doi.org/10.3389/fimmu.2025.1533044.

[43] J. Bladé, C. Fernández de Larrea, L. Rosiñol, Extramedullary disease in multiple myeloma in the era of novel agents, Br. J. Haematol. 169 (2015) 763–765, https://doi.org/10.1111/bjh.13384.

[44] A. Jurczyszyn, M. Olszewska-Szopa, V. Hungria, et al., Cutaneous involvement in multiple myeloma: a multi-institutional retrospective study of 53 patients, Leuk. Lymphoma 57 (2016) 2071–2076, https://doi.org/10.3109/10428194.2015.1128542.

[45] D. Zolnowski, S. Karp, P. Warncke, et al., Challenges in the treatment of soft-tissue plasmacytoma: a retrospective analysis of 120 patients with extramedullary multiple myeloma, J. Cancer Res. Clin. Oncol. 150 (2024) 482, https://doi.org/10.1007/s00432-024-05993-y.

[46] M. Cavo, E. Terpos, C. Nanni, et al., Role of 18F-FDG PET/CT in the diagnosis and management of multiple myeloma and other plasma cell disorders: a consensus statement by the International Myeloma Working Group, Lancet Oncol. 18 (2017) e206–e217, https://doi.org/10.1016/S1470-2045(17)30189-4.

[47] V. Montefusco, F. Gay, S. Spada, et al., Outcome of paraosseous extra-medullary disease in newly diagnosed multiple myeloma patients treated with new drugs, Haematologica 105 (2020) 193–200, https://doi.org/10.3324/haematol.2019.219139.

[48] J.P. Pintoffl, K. Weisel, M. Schulze, et al., Role of dynamic contrast-enhanced sonography for characterization and monitoring of extramedullary myeloma : Comparison with serologic data, J. Ultrasound Med. 32 (2013) 1777–1788, https://doi.org/10.7863/ultra.32.10.1777.

[49] C.L.B.M. Korst, C. O'Neill, W.S.C. Bruins, et al., Preclinical activity of allogeneic SLAMF7-specific CAR T-cells (UCARTCS1) in multiple myeloma, J. Immunother. Cancer 12 (2024), https://doi.org/10.1136/jitc-2023-008769.

[50] X. Zhang, Y.Y. Ng, Z. Du, et al., Vγ9Vδ2 T cells expressing a BCMA—Specific chimeric antigen receptor inhibit multiple myeloma xenograft growth, PLoS One 17 (2022), https://doi.org/10.1371/journal.pone.0267475.

[51] T.L.A. Wachsmann, M.H. Meeuwsen, D.F.G. Remst, et al., Combining BCMA-targeting CAR T cells with TCR-engineered T-cell therapy to prevent immune escape of multiple myeloma, Blood Adv. 7 (2023) 6178–6183, https://doi.org/10.1182/bloodadvances.2023010410.

[52] C.F. de Larrea, M. Staehr, A.V. Lopez, et al., Defining an optimal dual-targeted CAR T-cell therapy approach simultaneously targeting BCMA and GPRC5D to prevent BCMA escape–driven relapse in multiple myeloma, Blood Cancer Discov. 1 (2020) 146–154, https://doi.org/10.1158/2643-3230.BCD-20-0020.

[53] J.L. Thangaraj, S.Y. Ahn, S.H. Jung, et al., Expanded natural killer cells augment the antimyeloma effect of daratumumab, bortezomib, and dexamethasone in a mouse model, Cell. Mol. Immunol. 18 (2021) 1652–1661, https://doi.org/10.1038/s41423-021-00686-9.

[54] S. Okada, K. Vaeteewoottacharn, R. Kariya, Application of highly immunocompromised mice for the establishment of patient-derived xenograft (PDX) models, Cells 8 (2019), https://doi.org/10.3390/cells8080889.

[55] R. Mhaidly, E. Verhoeyen, Humanized mice are precious tools for preclinical evaluation of CAR T and CAR NK cell therapies, Cancers (Basel) 12 (2020) 1–22, https://doi.org/10.3390/cancers12071915.

[56] R.W.J. Groen, F.M. Hofhuis, H.-J. Prins, et al., The humanized multiple myeloma mouse model: opportunities for studying the pathogenesis of MM in its natural environment, Blood 114 (2009), https://doi.org/10.1182/BLOOD.V114.22.1847.1847, 1847–1847.

[57] W. Winkler, C.F. Díaz, E. Blanc, et al., Mouse models of human multiple myeloma subgroups, Proc. Natl. Acad. Sci. U. S. A. 120 (2023), https://doi.org/10.1073/PNAS.2219439120.
[58] M. Larrayoz, M.J. Garcia-Barchino, J. Celay, et al., Preclinical models for prediction of immunotherapy outcomes and immune evasion mechanisms in genetically heterogeneous multiple myeloma, Nat. Med. 29 (2023) 632–645, https://doi.org/10.1038/s41591-022-02178-3.
[59] T. Wang, Y. Yang, L. Ma, et al., BCMA-BBZ-OX40 CAR-T therapy using an instant manufacturing platform in multiple myeloma, J. Immunother. Cancer 12 (2024), https://doi.org/10.1136/jitc-2024-009476.
[60] Z.S. Hasanali, A.L. Garfall, L. Burzenski, et al., Human IL-6 fosters long-term engraftment of patient-derived disease-driving myeloma cells in immunodeficient mice, JCI Insight 9 (2024) e177300, https://doi.org/10.1172/JCI.INSIGHT.177300.
[61] J.M. Waldschmidt, S.J. Fruttiger, D. Wider, et al., Ex vivo propagation in a novel 3D high-throughput co-culture system for multiple myeloma, J. Cancer Res. Clin. Oncol. 148 (2022) 1045–1055, https://doi.org/10.1007/S00432-021-03854-6.
[62] W. Zhang, Y. Gu, Q. Sun, et al., Ex vivo maintenance of primary human multiple myeloma cells through the optimization of the osteoblastic niche, PLoS One 10 (2015) e0125995, https://doi.org/10.1371/JOURNAL.PONE.0125995.
[63] S. Richard, G. Lancman, A. Rossi, et al., Extramedullary relapse post CAR-T, Blood 140 (2022) 4301–4302, https://doi.org/10.1182/BLOOD-2022-170119.
[64] D. Pan, T.H. Mouhieddine, W. Fu, et al., Outcomes after CAR T cells in multiple myeloma patients with extramedullary and paramedullary disease, Blood 142 (2023), https://doi.org/10.1182/BLOOD-2023-177749, 1006–1006.
[65] Y. Qi, H. Li, K. Qi, et al., Clinical outcomes and microenvironment profiling in relapsed/refractory multiple myeloma patients with extramedullary disease receiving anti-BCMA CAR T-cell-based therapy, Am. J. Hematol. 99 (2024) 2286–2295, https://doi.org/10.1002/AJH.27469.
[66] D. Dima, A.O. Abdallah, J.A. Davis, et al., Impact of extraosseous extramedullary disease on outcomes of patients with relapsed-refractory multiple myeloma receiving standard-of-care chimeric antigen receptor T-Cell therapy, Blood Cancer J. 14 (2024), https://doi.org/10.1038/S41408-024-01068-W.
[67] C. Jin, R. Chen, S. Fu, et al., Long-term follow-up of BCMA CAR-T cell therapy in patients with relapsed/refractory multiple myeloma, J. Immunother. Cancer 13 (2025), https://doi.org/10.1136/JITC-2024-010687.
[68] H. Yao, S.H. Ren, L.H. Wang, et al., BCMA/GPRC5D bispecific CAR T-cell therapy for relapsed/refractory multiple myeloma with extramedullary disease: a single-center, single-arm, phase 1 trial, J. Hematol. Oncol. 18 (2025), https://doi.org/10.1186/S13045-025-01713-2.
[69] M.N. Kararoudi, Y. Nagai, E. Elmas, et al., CD38 deletion of human primary NK cells eliminates daratumumab-induced fratricide and boosts their effector activity, Blood 136 (2020) 2416–2427, https://doi.org/10.1182/BLOOD.2020006200.
[70] Y. Wang, H. Li, W. Xu, et al., BCMA-targeting bispecific antibody that simultaneously stimulates NKG2D-enhanced efficacy against multiple myeloma, J. Immunother. 43 (2020) 175–188, https://doi.org/10.1097/CJI.0000000000000320.
[71] A. Zhu, Y. Bai, Y. Nan, et al., Natural killer cell engagers: from bi-specific to tri-specific and tetra-specific engagers for enhanced cancer immunotherapy, Clin. Transl. Med. 14 (2024) e70046, https://doi.org/10.1002/ctm2.70046.